



**HAL**  
open science

## Electron counting and bonding patterns in assemblies of three and more silver-rich superatoms

F Gam, C W Liu, Samia Kahlal, J.-Y. Saillard

► **To cite this version:**

F Gam, C W Liu, Samia Kahlal, J.-Y. Saillard. Electron counting and bonding patterns in assemblies of three and more silver-rich superatoms. *Nanoscale*, 2020, 12 (39), pp.20308-20316. 10.1039/d0nr05179a . hal-02959823

**HAL Id: hal-02959823**

**<https://hal.science/hal-02959823v1>**

Submitted on 18 Nov 2020

**HAL** is a multi-disciplinary open access archive for the deposit and dissemination of scientific research documents, whether they are published or not. The documents may come from teaching and research institutions in France or abroad, or from public or private research centers.

L'archive ouverte pluridisciplinaire **HAL**, est destinée au dépôt et à la diffusion de documents scientifiques de niveau recherche, publiés ou non, émanant des établissements d'enseignement et de recherche français ou étrangers, des laboratoires publics ou privés.

# Electron counting and bonding patterns in assemblies of three and more silver-rich superatoms

Franck Gam<sup>a</sup>, C. W. Liu<sup>b</sup>, Samia Kahlal<sup>a</sup>, Jean-Yves Saillard<sup>a\*</sup>

\* Corresponding authors

<sup>a</sup> Université Rennes, CNRS, ISCR-UMR 6226, F-35000 Rennes, France

<sup>b</sup> Department of Chemistry, National Dong Hwa University, No. 1, Sec. 2, Da Hsueh Rd., Shoufeng, Hualien 974301, Taiwan

DFT calculations were carried out on a series of cluster cores, the framework of which being made of the condensation of several Pt@Ag<sub>12</sub> centered icosahedra. Icosahedra condensations through vertex-sharing, face-sharing and interpenetration were considered and their favored electron counts were determined from their stable closed-shell configurations. A large number of the computed assemblies of n icosahedral superatomic units can be considered as isolobal analogs of stable closed-shell n-atom molecules, most of them obeying the octet rule. The larger the degree of fusion between icosahedra, the stronger the interaction between them. It was for example possible to design 3-icosahedral supermolecular cores analogous to CO<sub>2</sub>, SF<sub>2</sub> or [I<sub>3</sub>], but also to the not yet isolated cyclic O<sub>3</sub>. Supermolecules equivalent to non-stable molecules can also be designed. Indeed, differences exist between atoms and superatoms, and original icosahedra assemblies with no “molecular” analog are also likely to exist, especially with compact structures and/or systems made of a large number of fused superatoms.

## 1. Introduction

When in low oxidation states, gold, silver and other late transition-metals tend to close-pack in a spherical way to give rise to stable species when “passivated” by a ligand protecting shell, which, in some cases, incorporates also metal centers in a higher oxidation state. The metal-metal bonding in such clusters was first rationalized by Mingos and coworkers<sup>1-6</sup> who pointed on the fact that it is dominated by the 6s gold orbitals and that their electron counts can be interpreted within the framework of the spherical jellium model.<sup>7</sup> This non-LCAO approach approximates the electron/nuclei interaction to a radial potential leading to the description of the electronic structure of such clusters in terms of jellium orbitals. The jellium orbitals somehow resemble atomic orbitals and extend substantially over the whole cluster sphere.

Table 1. Mingos’ analogy between diatomic molecules and gold clusters made of two fused centered icosahedra (adapted from Ref. 35). Pt atoms are in green. Encapsulated atoms are in green and shared atoms are in red. (a) The energy ordering of the occupied levels is arbitrary.

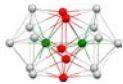
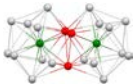
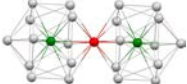
<b>Number of electrons</b>	10 = 2 × 8 – 6	12 = 2 × 8 - 4	14 = 2 × 8 - 2	16 = 2 × 8
<b>Diatomic molecule</b>	N <sub>2</sub>	O <sub>2</sub>	F <sub>2</sub>	Ne <sub>2</sub>
<b>Bond order</b>	3	2 (triplet state)	1	0 (van der Waals)
<b>Example of analogous cluster</b>	[Au <sub>17</sub> Ag <sub>2</sub> (NO <sub>3</sub> ) <sub>9</sub> (PMe <sub>2</sub> Ph) <sub>10</sub> ] <sup>+40</sup>	So far unknown	Au <sub>38</sub> (SR) <sub>24</sub> <sup>41</sup>	[Au <sub>13</sub> Ag <sub>12</sub> Br <sub>8</sub> (Ptol <sub>3</sub> ) <sub>10</sub> ] <sup>+33</sup>
<b>Electron configuration<sup>a</sup></b>	1σ <sub>g</sub> <sup>2</sup> 1σ <sub>u</sub> <sup>2</sup> 1π <sub>u</sub> <sup>4</sup> 2σ <sub>g</sub> <sup>2</sup> 1π <sub>g</sub> <sup>0</sup> 2σ <sub>u</sub> <sup>0</sup>	1σ <sub>g</sub> <sup>2</sup> 1σ <sub>u</sub> <sup>2</sup> 1π <sub>u</sub> <sup>4</sup> 2σ <sub>g</sub> <sup>2</sup> 1π <sub>g</sub> <sup>2</sup> 2σ <sub>u</sub> <sup>0</sup>	1σ <sub>g</sub> <sup>2</sup> 1σ <sub>u</sub> <sup>2</sup> 1π <sub>u</sub> <sup>4</sup> 2σ <sub>g</sub> <sup>2</sup> 1π <sub>g</sub> <sup>4</sup> 2σ <sub>u</sub> <sup>0</sup>	1σ <sub>g</sub> <sup>2</sup> 1σ <sub>u</sub> <sup>2</sup> 1π <sub>u</sub> <sup>4</sup> 2σ <sub>g</sub> <sup>2</sup> 1π <sub>g</sub> <sup>4</sup> 2σ <sub>u</sub> <sup>2</sup>
<b>Core structure</b>	interpenetrated 2 × 13 - 5 - 1 - 1 = 19 atoms  [Au <sub>17</sub> Ag <sub>2</sub> ] <sup>9+</sup>		face-sharing 2 × 13 - 3 = 23 atoms  [Au <sub>23</sub> ] <sup>9+</sup>	edge-sharing 2 × 13 - 1 = 25 atoms  [Au <sub>13</sub> Ag <sub>12</sub> ] <sup>9+</sup>

Table 2. Stable non-cyclic triatomic main group molecules.

Number of electrons	16 = 3 x 8 - 8	18 = 3 x 8 - 6	20 = 3 x 8 - 4	22 = 3 x 8 - 2	24 = 3 x 8
Triatomic systems	CO <sub>2</sub> , [N <sub>3</sub> ] <sup>-</sup>	SO <sub>2</sub> , [NO <sub>2</sub> ] <sup>-</sup>	SF <sub>2</sub>	XeF <sub>2</sub> , [I <sub>3</sub> ] <sup>-</sup>	3I <sup>-</sup> , 3Ne
Bond order	2	1.5	2	0.5	0 (van der Waals)
Bond angle	linear (sp)	bent (sp <sup>2</sup> )	bent (sp <sup>3</sup> )	linear	-

Their shell ordering spans as  $1S < 1P < 1D < 2S < 1F < 2P...$  As for atomic systems, closed-shell (noble gas-like) stability is achieved for specific (so-called “magic”) electron counts, spanning 2, 8, 18, 20, 34, 40... Such an atom-like description of clusters was conceptualized as the superatom model<sup>8-11</sup> and the jellium orbitals are often called superatomic orbitals. One of the most frequent close-packed spherical motif encountered in group 11 cluster chemistry is the centered icosahedron,<sup>12-17</sup> which is generally associated with the 8-electron “magic” number. Typical group 11 examples are [Au<sub>25</sub>(SR)<sub>18</sub>]<sup>-</sup><sup>13,14,18,19</sup> and [Ag<sub>21</sub>(dtp)<sub>12</sub>]<sup>+</sup> (dtp = dithiophosphate = S<sub>2</sub>P(OR)<sub>2</sub>).<sup>15</sup> Both species can be viewed as made of an [M<sub>13</sub>]<sup>5+</sup> (M = Au, Ag) centered icosahedral superatomic core (8 s-type valence electrons) stabilized by a “passivating shell” made of 18 [SR]<sup>-</sup> ligands and 12 Au<sup>+</sup> atoms in the former case, and 12 [S<sub>2</sub>P(OR)<sub>2</sub>]<sup>-</sup> ligands and 8 Ag<sup>+</sup> atoms in the latter case. In both systems, the outer M<sup>+</sup> atoms interact weakly with the [M<sub>13</sub>]<sup>5+</sup> core, but are strongly coordinated to sulphur lone pairs, making locally stable linear 14-electron or trigonal planar 16-electron d<sup>10</sup> metal centers.

Of course, many late transition-metal clusters, especially high nuclearity species, are not spherical and consequently their electronic structure cannot be rationalized within the spherical jellium model. At the end of the last century, Teo and coworkers proposed the concept of clusters of clusters<sup>20,21</sup> for describing the non-spherical metallic cores of group 11 clusters made of vertex-sharing centered icosahedra. A question that arises then is: can we look at assemblies of superatoms in the same way as one looks at assemblies of atoms, i.e. molecules. In other words, in the same way as, for example, the 14-electron F<sub>2</sub> molecule is made of two atoms of valence configuration 2s<sup>2</sup> 2p<sup>5</sup>, is there a stable closed-shell isolobal<sup>22</sup> equivalent cluster, made of two fused superatoms, each of them of jellium configuration 1S<sup>2</sup> 1P<sup>5</sup>? It turns out that the answer to this question lies already in the literature. Several authors have described the electronic structure of real or hypothetical clusters made of two fused superatoms as analogous to that of diatomic molecules.<sup>23-37</sup> As regards gold-rich clusters made of two fused centered icosahedra, an illuminating rationalization of their electron counts was proposed by Mingos in 2015.<sup>35</sup> Its major conceptual developments are summarized in Table 1. One can see that an important parameter affecting the cluster electron count is its degree of fusion (vertex-sharing, face-sharing or interpenetrating), in a similar way as the bond order does for main group molecules.

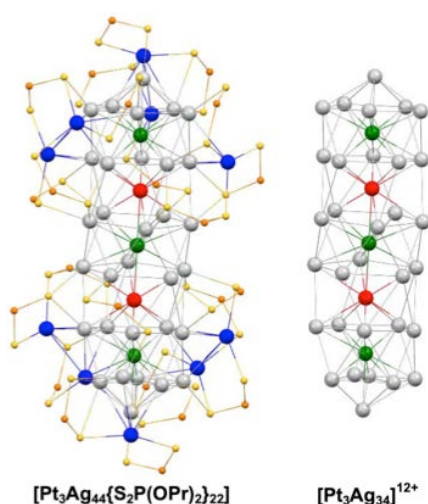


Figure 1. Left: The structure of  $[\text{Pt}_3\text{Ag}_{44}(\text{S}_2\text{P}(\text{OPr})_2)_{22}]$  (OPr groups omitted for clarity); right: Its 22-electron  $[\text{Pt}_3\text{Ag}_{34}]^{12+}$  tricosahedral core isolobal to  $[\text{I}_3]^-$  (from ref. 38).

To our knowledge, apart from a pioneering limited case study,<sup>39</sup> no systematic investigation of electron counting and electronic structure of late transition-metal clusters made of the condensation of more than two superatoms has been made so far. Recently, we published the synthesis, characterization and electronic structure of the tricosahedral cluster  $\text{Pt}_3\text{Ag}_{44}(\text{dtp})_{22}$  (Figure 1).<sup>38</sup> Its core structure is a linear assembly of three  $\text{Pt}@Ag_{12}$  icosahedra sharing two Ag vertices. Our density functional theory (DFT) calculations indicated that this 22-electron species is an isolobal analog of the linear  $[\text{I}_3]^-$  ion. In this paper we extend our investigation to the possibility for various fused tris-icosahedral structures adopting favored closed-shell electron counts that would render them analogous to regular stable triatomic molecules (Table 2). Tetra-icosahedral and some larger assemblies are subsequently considered.

## 2. Computational Details

All calculations were carried out at the DFT level with the Amsterdam Density Functional (ADF) program.<sup>42</sup> The gradient-corrected Becke-Perdew (BP86) exchange correlation functional<sup>43,44</sup> was used, together with the triple- $\zeta$ , plus two polarization functions (STO-TZ2P) Slater type basis set. The zeroth-order regular approximation (ZORA) was employed in the calculations to account for scalar relativistic effects.<sup>45</sup> The frozen core approximation was applied to the  $[1s^2-4f^{14}]$  inner electrons for Pt and Au, and  $[1s^2-4p^6]$  for Ag. Geometry optimizations were performed assuming a maximum cartesian step smaller than  $10^{-3}$  Å and an energy convergence criterion of  $10^{-5}$  Ha. Owing to the fact that the computed cluster cores are highly charged cations, solvent effects through the conductor-like screening model (COSMO)<sup>46,47</sup> was considered, to mimic the effects of counterions. Such a process has been proved to be efficient to treat metal cations.<sup>48</sup> The considered solvent was dichloromethane.

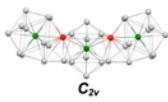
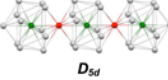
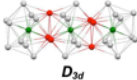
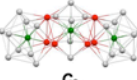
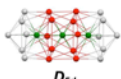
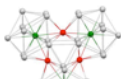
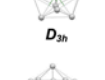
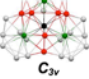
	Favored count	$d_{\text{Pt-Pt}}$	$\Delta E_{\text{H-L}}$	Isolobal to
 $C_{2v}$	24e [Pt <sub>3</sub> Ag <sub>34</sub> ] <sup>10+</sup>	5.636 Å	0.6 eV	3Ne
 $D_{5d}$	24e [Pt <sub>3</sub> Ag <sub>34</sub> ] <sup>10+</sup>	5.621 Å	0.5 eV	3Ne
	22e [Pt <sub>3</sub> Ag <sub>34</sub> ] <sup>12+</sup>	5.464 Å	1.0 eV	I <sub>3</sub> <sup>-</sup>
 $D_{3d}$	22e [Pt <sub>3</sub> Ag <sub>30</sub> ] <sup>8+</sup>	4.507 Å	1.1 eV	I <sub>3</sub> <sup>-</sup>
 $C_{2v}$	20e [Pt <sub>3</sub> Ag <sub>30</sub> ] <sup>10+</sup>	4.419 Å	0.8 eV	SF <sub>2</sub>
 $D_{5d}$	16e [Pt <sub>3</sub> Ag <sub>22</sub> ] <sup>6+</sup>	2.752 Å	0.9 eV	CO <sub>2</sub>
 $D_{3h}$	24e [Pt <sub>3</sub> Ag <sub>33</sub> ] <sup>9+</sup>	5.649 Å	0.7 eV	3Ne
 $C_{3v}$	18e [Pt <sub>3</sub> Ag <sub>24</sub> ] <sup>10+</sup>	4.447 Å	1.0 eV	triangular O <sub>3</sub>
 $D_{3h}$	20e [Pt <sub>3</sub> Ag <sub>20</sub> ]	2.723 Å	0.7 eV	-

Figure 2. Stable closed-shell assemblies of three fused icosahedra ( $\Delta E_{\text{H-L}}$  = HOMO-LUMO gap). Pt atoms are in green. Silver atoms in red and black are shared between 2 and 3 icosahedra, respectively.

### 3. Results and Discussion

#### 3.1. Assembling three icosahedra

We have shown previously that computing the only superatomic core of a cluster in its actual oxidation state, i.e. without its passivating shell, allows rationalizing the cluster electronic structure in terms of a superatom or assembly of superatoms.<sup>15,38</sup> Below we report our search for cluster cores made of three fused Pt@Ag<sub>12</sub> icosahedral units that would be closed-shell energy minima secured by significant HOMO-LUMO gaps ( $\geq 0.5$  eV, unless specified in the text). The Pt@Ag<sub>12</sub> unit is that encountered in our first characterized tris-icosahedral cluster. Test calculations on isoelectronic structures made of Ag@Ag<sub>12</sub> units provided similar results. On the other hand, the presence of Pt at the icosahedra centers helps reducing the cationic charge of the computed models. Thus, two parameters were varied. One is the degree of icosahedra condensation: vertex-sharing, face-sharing and interpenetration. Edge-sharing was discarded owing to the fact that, to our knowledge, no experimental report exists. The other parameter is the electron count, i.e. the cluster charge.

**3.1.1. Vertex-sharing.** There are two different open triangular configurations possible, depending which ones are the two vertex type that the central icosahedron shares with its two congeners: second or third neighbors (sharing two first neighbors would lead to a cyclic structure; see below). Assuming ideal assemblies of ideal icosahedra, they would correspond to Pt-Pt-Pt angles of 117° and 180°, respectively. The low degree of icosahedra condensation lets to expect weak interaction between them, thus large electron counts. Indeed, the only favored electron counts were found to be 22

and 24. The 24-electron count corresponds to the trivial case of three non-interacting saturated 8-electron superatoms, thus isolobal to a system made of three van der Waals bonded Ne atoms (Table 2). The lowest energy configuration (Figure 2) is bent, i.e. the two shared vertices of the central icosahedron are second neighbors. Interestingly, the Pt-Pt-Pt angle ( $137^\circ$ ) is much larger than the ideal value of  $117^\circ$ . This is because the (Ag-Pt-Ag-Pt-Ag-Pt-Ag) backbone is also bent at the shared Ag atoms ( $160^\circ$ ). It results that the outer and central icosahedra have short Ag...Ag contacts ( $2.90 \text{ \AA}$ ) on one side (top side of bent  $[\text{Pt}_3\text{Ag}_{34}]^{10+}$  in Figure 2) and much longer ones ( $3.94 \text{ \AA}$ ) on the other side (bottom side of bent  $[\text{Pt}_3\text{Ag}_{34}]^{10+}$  in Figure 2). The absence of backbone bending at the Ag atoms would have resulted in all-equal inter-icosahedral Ag...Ag contacts of  $\sim 3.4 \text{ \AA}$ .

The linear (Pt-Pt-Pt =  $180^\circ$ ) 24-electron isomer is found to lie only 4.5 kcal/mol above the bent one (Figure 2). It is thus likely that for this electron count the bent vs. linear arrangement is going to be largely dependent on the structural requirements of the passivating shell. In fact, to our knowledge only one 24-electron vertex-sharing species has been characterized so far, namely  $[\text{Au}_{37}(\text{PPh}_3)_{10}(\text{SC}_2\text{H}_4\text{Ph})_{10}\text{X}_2]^+$  (X = Cl<sup>-</sup> or Br<sup>-</sup>)<sup>49,50</sup>. Its superatomic core adopts the linear arrangement.

The linear configuration was found to be the most stable in the case of the 22-electron count (Figure 2). We previously showed that such a species is isolobal to the linear  $[\text{I}_3]^-$  anion.<sup>38</sup> Figure 3 illustrates the correspondence between the  $[\text{I}_3]^-$  MOs and the  $[\text{Pt}_3\text{Ag}_{34}]^{12+}$  “supermolecular” orbitals. The former are linear combinations of atomic orbitals and the latter are combinations of superatomic orbitals. Consistently with the rather large 22-electron count, the bent configuration lies only 3 kcal/mol above the linear one. As mentioned previously, the linear  $[\text{Pt}_3\text{Ag}_{34}]^{12+}$  is the superatomic core of the fully characterized  $\text{Pt}_3\text{Ag}_{44}(\text{dtp})_{22}$  (Figure 1).<sup>38</sup> To our knowledge, no other 22-electron species has been mentioned so far.

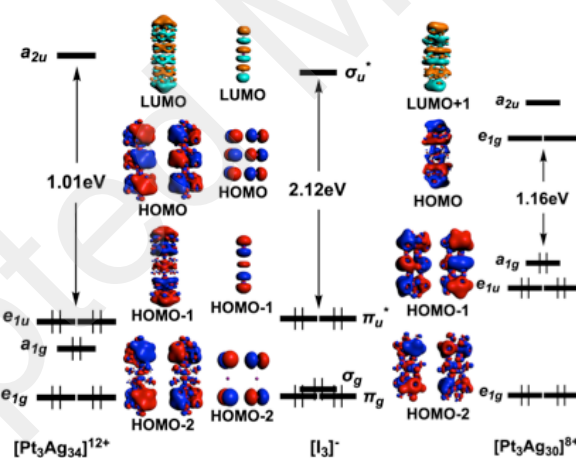


Figure 3. Kohn–Sham orbital diagrams of the 22-electron  $[\text{Pt}_3\text{Ag}_{34}]^{12+}$  ( $D_{5d}$ , left),  $[\text{Pt}_3\text{Ag}_{30}]^{8+}$  ( $D_{3d}$ , right), and  $[\text{I}_3]^-$  ( $D_{\infty h}$ , middle). The HOMOs of  $[\text{I}_3]^-$  are the  $\pi^*$  orbitals and the LUMO is the unique vacant  $\sigma^*$  orbital.

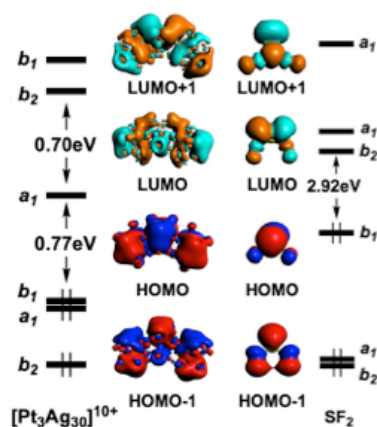


Figure 4. Kohn-Sham orbital diagrams of the  $C_{2v}$ , 20-electron  $[\text{Pt}_3\text{Ag}_{30}]^{10+}$  and  $\text{SF}_2$ . The HOMO and HOMO-1 of  $\text{SF}_2$  are the  $\pi$ -type and  $\sigma$ -type S "lone pairs". The LUMO and LUMO+1 are the  $\sigma^*(\text{S-F})$  orbitals.

An equilateral triangular structure can be generated from the assembly of three vertex-sharing icosahedra when the two shared vertices of each icosahedron are first neighbors. For such a  $D_{3h}$   $\text{Pt}_3\text{Ag}_{33}$  framework (Figure 2), only one favored closed-shell situation was found, corresponding to 24 electrons, i.e., three non-interacting 8-electron superatoms. It turns out that this vertex-sharing triangular architecture has been reported for five related 24-electron clusters, namely  $[(p\text{-Tol}_3\text{P})_{12}\text{Au}_{18}\text{Ag}_{20}\text{Cl}_{14}]$ ,  $[(\text{Ph}_3\text{P})_{14}\text{Au}_{18}\text{Ag}_{20}\text{Cl}_{12}]^{2+}$ ,  $[\text{Cu}_3\text{Au}_{34}(\text{PPh}_3)_{13}(\text{tBuPhCH}_2\text{S})_6\text{S}_2]^{3+}$ ,  $[\text{Pt}_3\text{Ag}_{33}(\text{PPh}_3)_{12}\text{Cl}_8]^+$  and  $[\text{Pt}_3\text{Ag}_{21}\text{Au}_{12}(\text{PPh}_3)_{12}\text{Cl}_8]^+$  <sup>20,21,29,51,52</sup>.

**3.1.2. Face-sharing.** With face-sharing icosahedra there are three non-cyclic configurations that are possible for a  $\text{Pt}_3\text{Ag}_{30}$  ( $30 = 3 \times 12 - 6$ ) core, depending which faces of the central icosahedron are shared and without leading to steric overcrowding. Assuming ideal assemblies of ideal icosahedra, they would correspond to Pt-Pt-Pt angles of  $109^\circ$ ,  $138^\circ$  and  $180^\circ$ , respectively. The linear configuration was found to be favored for the unique 22-electron count (Figure 2), thus making this cluster core isolobal to  $[\text{I}_3]^-$ , as illustrated in Figure 3). For this electron count, the bent configurations are significantly disfavored. The 20-electron count is found to be favored for the bent configuration corresponding to an ideal Pt-Pt-Pt angle of  $138^\circ$ , the optimized value being  $140^\circ$  (Figure 2). This cluster core is isolobal to  $\text{SF}_2$ , as illustrated in Figure 4.

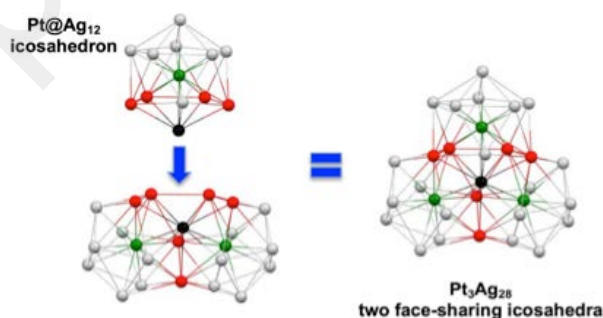


Figure 5. The making of a  $C_{3v}$  cyclic  $\text{Pt}_3\text{Ag}_{28}$  framework by the fusion of a  $\text{Pt}@\text{Ag}_{12}$  icosahedron to a  $\text{Pt}_2\text{Ag}_{21}$  unit made of 2 edge-sharing icosahedra. Pt atoms are in green. Silver atoms in red and black are shared between 2 and 3 icosahedra, respectively.

It is possible to build an equilateral assembly of three (slightly distorted) icosahedra by adding one supplementary icosahedron to a framework made of two face-sharing icosahedra as illustrated in Figure 5. In the resulting  $C_{3v}$   $\text{Pt}_3\text{Ag}_{28}$

assembly, three faces are shared, of which one vertex is common to the 3 icosahedra ( $31 = 3 \times 13 - 3 \times 3 + 1$ ). Its favored electron count was found to be 18 (Figure 2), i.e. that of the elusive high-energy isomer of  $O_3$ ,<sup>53-57</sup> or more prosaically that of cyclopropane. Its MO diagram (Figure 6) is consistent with this  $O_3$  analogy.

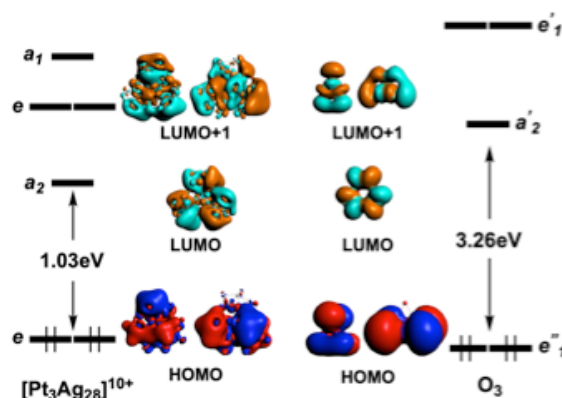


Figure 6. Kohn-Sham orbital diagrams of the 18-electron  $[Pt_3Ag_{28}]^{10+}$  ( $C_{3v}$ ) and hypothetical cyclic  $O_3$  isomer ( $D_{3h}$ ). The HOMOs of  $O_3$  are the  $\pi^*$  combinations and the three LUMOs are the vacant  $\sigma^*$  orbital.

### 3.1.3. Interpenetration of icosahedra and the relationship with vertex-sharing.

Two interpenetrated centered icosahedra (Figure 7, left) share a five-vertex pentagonal ring, as well as an icosahedron center which is a vertex for the other one, and conversely. There are two ways of adding a third interpenetrating centered icosahedron to get a  $Pt_3Ag_{22}$  non-cyclic framework, as illustrated on the right side of Figure 7.

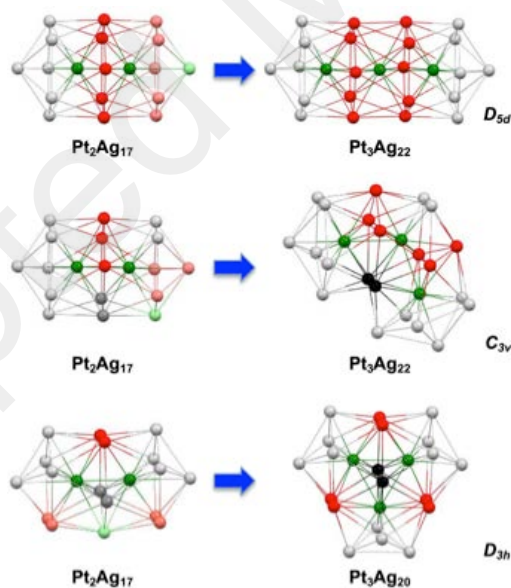


Figure 7. The two ways of making of a non-cyclic (top and middle) and cyclic (bottom)  $Pt_3Ag_{22}$  framework resulting from the interpenetration of a supplementary icosahedron to a bisicosahedral  $Pt_2Ag_{17}$  unit (2 interpenetrating icosahedra). Pt atoms are in green. Silver atoms in red and black are shared between 2 and 3 icosahedra, respectively.

In fact, as already pointed out a long time ago by Teo,<sup>33</sup> the linear  $D_{5d}$  25-atom framework of Figure 7 is nothing else than the 25-atom vertex-sharing bisicosahedral arrangement of Table 1. Removing the connection lines between the facing red pentagons of the former structure would produce that of the latter. Assuming ideally staggered ideal icosahedra,



the bisicosahedral structure of Table 1 would correspond to inter-icosahedra distances equal to only 1.18 times the icosahedra edge. Since the structure has not so much spatial flexibility to adjust these distances, both views (2 vertex-sharing centered icosahedra and 3 interpenetrated centered icosahedra) can be considered as two different descriptions of the same geometrical object. As a matter of fact, the favored electron count of the  $D_{5d}$   $\text{Pt}_3\text{Ag}_{22}$  model of Figure 7 is the same as that of the vertex-sharing bisicosahedral structure of Table 1, namely 16 electrons (Figure 1). Thus,  $[\text{Pt}_3\text{Ag}_{22}]^{6+}$  can be viewed as either isolobal to the  $\text{Ne}_2$  van der Waals dimer (two vertex-sharing superatoms) or to  $\text{CO}_2$  (three interpenetrated superatoms). The two approaches are not excluding each other since both  $\text{Ne}_2$  and  $\text{CO}_2$  have similar valence electron configurations in the way that their 16 electrons occupy the same number of  $\sigma_g$  (two),  $\sigma_u$  (two),  $\pi_g$  (one) and  $\pi_u$  (one) levels. The compactness of the central icosahedron is a reasonable geometrical indicator for choosing the most appropriate description. In the case of our  $D_{5d}$   $[\text{Pt}_3\text{Ag}_{22}]^{6+}$  model (Figure 2), the contacts between the two outer icosahedra (3.165 Å) are less than 1.1 times the outer icosahedra edges, indicative of significant compactness of the central icosahedron and therefore favoring the isolobal analogy with  $\text{CO}_2$  that is illustrated in (Figure 8).

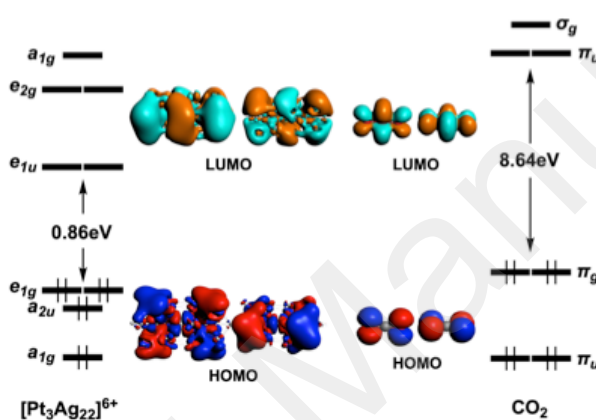


Figure 8. Kohn-Sham orbital diagrams of the 16-electron  $[\text{Pt}_3\text{Ag}_{22}]^{6+}$  core and  $\text{CO}_2$ .

It is of note that in the isoelectronic and isostructural  $D_{5d}$   $[\text{Pt}_2\text{Ag}_{23}]^{7+}$  model, generated by simply replacing the central Pt atom of  $[\text{Pt}_3\text{Ag}_{22}]^{6+}$  by  $\text{Ag}^+$ , the contacts between the two outer icosahedra (3.318 Å) are 1.14 times the outer icosahedra edges. This is indicative of a weaker compactness, thus somehow favoring the analogy with  $\text{Ne}_2$ . This model actually constitutes the core of the structurally characterized 16-electron cluster  $\text{Pt}_2\text{Ag}_{33}(\text{dtp})_{17}$ .<sup>38</sup>

The above analogy between a staggered vertex-sharing bisicosahedral unit and a structure made of three interpenetrating icosahedra can be extended to any linear  $n$ -vertex sharing framework, which can be described as made of  $2n - 1$  interpenetrating icosahedra. The 24-electron linear tris-icosahedral structure  $[\text{Pt}_3\text{Ag}_{34}]^{10+}$  described above can then be viewed as either the isolobal analog to a  $\text{Ne}_3$  van der Waals molecule or to carbon suboxide  $\text{O}=\text{C}=\text{C}=\text{O}$ . Interestingly, the linear 22-electron  $[\text{Pt}_3\text{Ag}_{34}]^{12+}$  (Figure 2) has no simple 5-atom main-group stable analog. The analogy of linear  $n$ -icosahedral vertex sharing structures with linear  $2n - 1$  main-group atom linear molecules works preferentially for  $8n$ -electron species.

It is possible to build an equilateral assembly of three interpenetrating icosahedra by adding one supplementary icosahedron to a framework made of two interpenetrating icosahedra as illustrated at the bottom of Figure 7. The resulting  $\text{Pt}_3\text{Ag}_{20}$  architecture has  $D_{3h}$  symmetry. This 23-atom structure has been shown to constitute the core of the  $\text{Pd}_{37}(\text{CO})_{28}\{\text{P}(\text{p-Tolyl})_3\}_{12}$  nanocluster.<sup>58</sup> For this arrangement, the unique favored closed-shell electron count is 20, i.e.  $[\text{Pt}_3\text{Ag}_{20}]$ . There is no isoelectronic triatomic molecular equivalent. On the other hand, 20 is a “magic” closed-shell superatom electron number, corresponding to the  $1\text{S}^2 1\text{P}^6 1\text{D}^{10} 2\text{S}^2$  configuration. It turns out that this is a quite compact structure, although its shape is

somehow non-spherical (oblate-distorted). It exhibits an MO diagram (Figure 9) consistent with this view, with a 1D HOMO and a LUMO of 1F lineage. In this particular case, the 2S orbital lies below the 1D block.

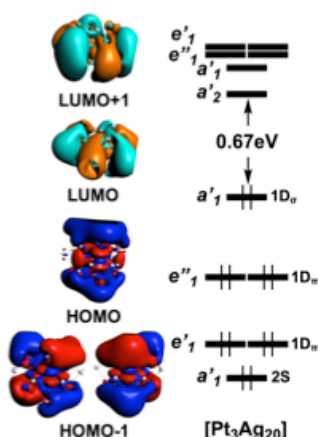


Figure 9. Kohn-Sham orbital diagram of the  $D_{3h}$  20-electron  $[\text{Pt}_3\text{Ag}_{20}]$ .

### 3.2. Assembling more than three icosahedra.

The number of configurational possibilities to generate assemblies of four (or more) icosahedra is very large. This is why we have limited our investigation to the linear and star-shaped (one central icosahedron connected to three outer congeners) assemblies of four  $\text{Pt@Ag}_{12}$  units, in order to verify that the analogy with simple main-group molecules holds also for larger systems. Thus, six structures were generated, depending on whether the four icosahedra are vertex-sharing, face-sharing or interpenetrating. They are depicted in Figure 10, together with their favored electron counts and their Kohn-Sham orbital diagrams are provided in Figure S1. As expected, the  $32 = 4 \times 8$  count is compatible with the two vertex-sharing structures (linear and star-shaped), since it is consistent with weakly interacting closed-shell superatoms. Interestingly, the linear configuration is also favorable to the lower 30-electron count ( $[\text{Pt}_4\text{Ag}_{45}]^{15+}$ ). Examination of its electronic structure indicates that it is isolobal to the linear 30-electron tetraiodide anion  $[\text{I}_4]^{2-}$ .<sup>59</sup> This is in line with the results obtained for the one-icosahedron shorter linear  $[\text{Pt}_3\text{Ag}_{34}]^{12+}$  model (Figure 2), which is isolobal to  $[\text{I}_3]^-$ . The 30-electron ligated model  $[\text{Pt}_4\text{Ag}_{55}(\text{S}_2\text{PH}_2)_{27}]^{2-}$ , which contains the  $[\text{Pt}_4\text{Ag}_{45}]^{15+}$  core, and built as an extrapolation of  $[\text{Pt}_3\text{Ag}_{44}(\text{S}_2\text{P}(\text{OPr})_2)_{22}]$  (Figure 1) with one more repeat unit, provided the same electronic structure as its  $[\text{Pt}_4\text{Ag}_{45}]^{15+}$  core; with a comparable substantial HOMO-LUMO gap of 0.72 eV (Figure S2).

The two investigated face-sharing models were found having the same unique 28-electron favored count  $[\text{Pt}_4\text{Ag}_{39}]^{11+}$  (Figure 10). The star-shaped framework is isolobal to hypervalent tetrahalogenides such as  $\text{ClF}_3$ . The linear form has a more intriguing electronic structure which could be tentatively described as an analogue to an hypothetical linear  $\text{I}_4$  hypervalent species, in which the two bonding electron pairs are delocalized over three bonding contacts.

The favored electron count for the linear  $[\text{Pt}_4\text{Ag}_{27}]^{5+}$  model with interpenetrating icosahedra is 22. Examination of its Kohn-Sham orbitals indicates it is the analog of a hypothetical linear  $[\text{N}_4]^{2-}$  ion 60 (isoelectronic to  $\text{C}_2\text{F}_2$ ). The star-shaped framework has a favored count of 20 electrons and an electronic structure related to that of the trimethylene methane dication, but, unlike the latter, with high-lying vacant  $\pi$ -type orbitals.

To our knowledge, none of the cluster cores shown in Figure 10 have been experimentally evidenced, so far. A few larger superatom assemblies have been however characterized by Zhu and collaborators.<sup>61,62</sup> One of them is  $[\text{Au}_{60}\text{Se}_2(\text{Ph}_3\text{P})_{10}(\text{SePh})_{15}]^+$ .<sup>61</sup> the metal framework of which consists of the cyclic assembly of five vertex-sharing icosahedra.

This  $[\text{Au}_{60}]^{20+}$  ring of icosahedra possesses  $40 = 8 \times 5$  electrons, i.e. exhibits weak interactions between the superatoms, as previously demonstrated by Lin and coworkers.<sup>39</sup> It is the so far largest element of the family of  $8n$ -electron clusters made of  $n$  vertex-sharing icosahedra. Another recently published cluster from this group, namely  $[\text{Au}_8\text{Ag}_{57}(\text{Dppp})_4(\text{C}_8\text{H}_{11}\text{S})_{33}\text{Cl}_2]^+$  ( $\text{Dppp}$  = diphenylphosphinepropane)<sup>62</sup> appears much more intriguing. This 30-electron cluster possesses an  $\text{Au}_8\text{Ag}_{41}$  inner core of ideal  $D_{2d}$  symmetry that can be described as a cyclic assembly of eight interpenetrating  $\text{Au}@Ag_{12}$  icosahedra (left side of Figure 11). It is a 49-atom metal core because the silver atom at the center is shared by the eight icosahedra ( $49 = 13 \times 8 - 8 \times 7 + 1$ ).

We performed calculations on the 30-electron  $[\text{Au}_8\text{Ag}_{41}]^{19+}$  core and on a simplified model of  $[\text{Au}_8\text{Ag}_{57}(\text{Dppp})_4(\text{C}_8\text{H}_{11}\text{S})_{33}\text{Cl}_2]^+$  in which the phenyl and cyclohexyl groups were replaced by methyl substituents. Their computed HOMO-LUMO gaps are similar (0.60 and 0.47 eV, respectively). Both systems have related electronic structures, confirming the qualitative description of  $[\text{Au}_8\text{Ag}_{57}(\text{Dppp})_4(\text{C}_8\text{H}_{11}\text{S})_{33}\text{Cl}_2]^+$  as made of a  $[\text{Au}_8\text{Ag}_{41}]^{19+}$  core “passivated” by an inner shell made of 4  $\text{Dppp}$ , 33  $(\text{C}_8\text{H}_{11}\text{S})^-$ , 2  $\text{Cl}^-$  and 16  $\text{Ag}^+$ . The question that arises then is how to rationalize the 30-electron count of the metal core. No simple 8-member cyclic molecule has this electron count.

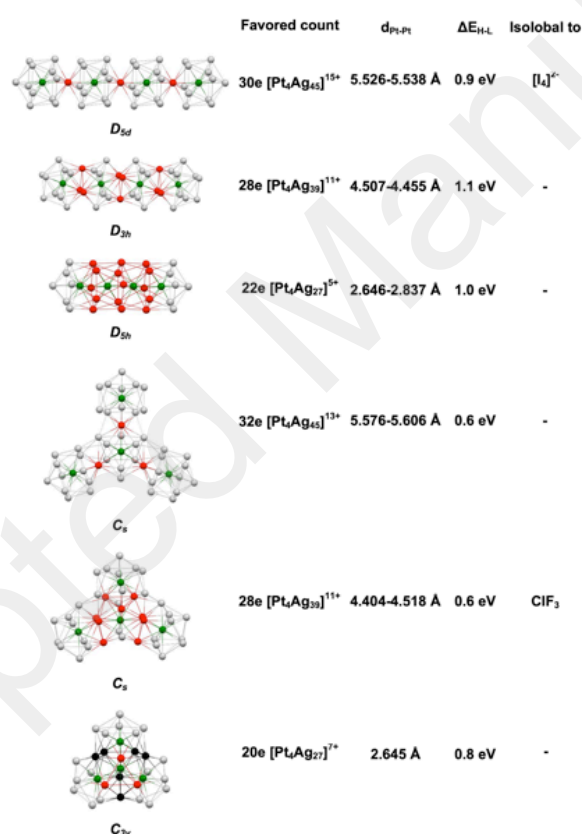


Figure 10. Summary of different tetra-icosahedra linear and propeller assemblies. Pt atoms are in green. Silver atoms in red and black are shared between 2 and 3 icosahedra, respectively.

Cyclooctatetraene, for example, is a 40-electron system. Looking at the whole  $[\text{Au}_8\text{Ag}_{41}]^{19+}$  as a spherical superatom (as for  $D_{3h} [\text{Pt}_3\text{Ag}_{20}]$ , see above) is not helpful since 40 is not a “magic” number within the spherical jellium model. This is not surprising, owing to the substantially flattened (oblate) shape. On the other hand, 30 is a “magic” number within the approximation of the planar (2D) harmonic quantum dot model.<sup>63</sup> This would correspond to the  $1S^2 1P^4 1D^4 2S^2 2P^4 1F^4 1G^4 2D^4 3S^2$ . It should be noted that the planar approximation, no  $\pi$ -type P, D, F or G orbital is considered (shells closed with 4 electrons). It turns out that the expected 2D and 3S orbitals are missing within the occupied orbitals of

$[\text{Au}_8\text{Ag}_{41}]^{19+}$  (Figure 11, right side). Rather, the  $\pi$ -type  $1P_z$  and  $1D_{xz,yz}$  components appear among them, conferring the cluster with 6-electron  $\pi$ -type aromaticity. The jellium configuration can be written as  $1S^2 1P_{\sigma+\pi}^6 1D_{\sigma+\pi}^8 2S^2 2P_{\sigma}^4 1F_{\sigma}^4 1G_{\sigma}^4$ .

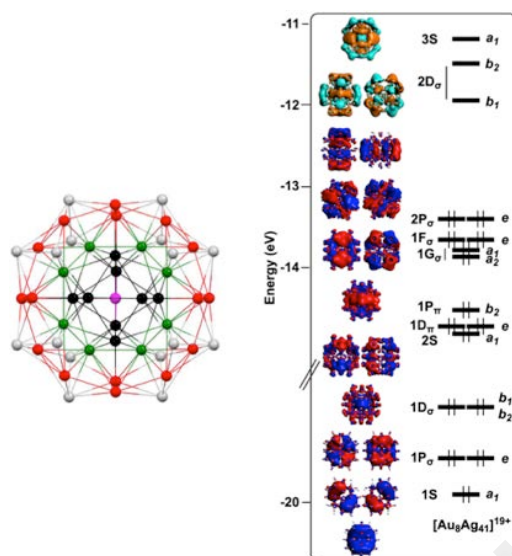


Figure 11. left side: The  $[\text{Au}_8\text{Ag}_{41}]_{19+}$  core of  $[\text{Au}_8\text{Ag}_{57}(\text{Dppp})_4(\text{C}_8\text{H}_{11}\text{S})_{33}\text{Cl}_2]^+$  (from ref. 62), made of eight interpenetrating icosahedra (ideal  $D_{2d}$  symmetry). Au atoms are in green and occupy the icosahedra centers. Silver atoms in red, black and magenta are shared between 2, 3 and 8 icosahedra, respectively. Right side: Its Kohn-Sham orbital diagram.

Clearly, one is in an intermediate situation between the spherical (3D) and planar (2D) jellium approximation. As regard electronic structure, some relationship can also be drawn with planar boron clusters.<sup>64,65</sup> Although this structure is likely to be unique, one can anticipate that other architectures exhibiting important oblate or prolate distortion could be stabilized with specific jellium electron counts.

#### 4. Conclusions

Our DFT calculations on various assemblies of  $n$  icosahedral superatomic units ( $n > 2$ ) confirm that it is possible to conceive stable closed-shell supermolecules that would be analogs to stable  $n$ -atomic molecules, most of them obeying the octet rule. The larger the degree of fusion between icosahedra, the stronger the interaction between them. It is also possible to design stable superatomic assemblies that can be analogous to unknown molecules, as exemplified by  $[\text{Pt}_3\text{Ag}_{28}]^{10+}$  ( $C_{3v}$ ) which is the analog of the not yet isolated cyclic ozone isomer.<sup>56,57</sup> Supermolecules equivalent to non-stable molecules could also be designed, such as  $[\text{Pt}_4\text{Ag}_{27}]^{5+}$  which is the analog of linear  $[\text{N}_4]^{2-}$  ion, whose relaxed structure is bent. In any case, the atom/superatom equivalence should not be taken too far. There are differences and these differences add up when the number of considered atoms/superatoms increases. This can be also the case for ring structures. In general, cyclic molecules have no appreciable density at their center. Because of their size and depending on their degree of fusion, cyclic assemblies of icosahedra can extend their atomic framework at (or near) the center of the ring, thus forcing delocalization across the ring. In such a case, the molecule/supermolecule equivalence does not hold anymore. The whole cluster framework is better described as a superatom per se. This is the case of our  $D_{3h}$  20-electron  $[\text{Pt}_3\text{Ag}_{20}]$  model, for example. Such compact assemblies of fused icosahedra can importantly deviate from spherical shape, as for example the  $[\text{Au}_8\text{Ag}_{41}]^{19+}$  inner core of the experimentally characterized  $[\text{Au}_8\text{Ag}_{57}(\text{Dppp})_4(\text{C}_8\text{H}_{11}\text{S})_{33}\text{Cl}_2]^+$  nanocluster. With its

specific degree of oblativity, this 30-electron species has a specific closed-shell electron count. We hope that this work will encourage efforts to grow ligand-protected poly-icosahedral clusters and open new opportunities for practical experimentations.

## Conflicts of interest

There are no conflicts to declare.

## Acknowledgements

This work was supported by the France-Taiwan ANR-MOST 2018 program (projectNanoalloys) and Ministry of Science and Technology in Taiwan (MOST 108-2923-M-259-001). The GENCI is acknowledged for HPC resources (Project A0050807367).

## Notes and references

1. D. M. P. Mingos, *J. Chem. Soc., Dalton Trans.*, 1976, 1163-1169.
2. D. M. P. Mingos, *J. Chem. Soc., Chem. Commun.*, 1985, 1352-1354.
3. D. M. P. Mingos and R. L. Johnston, *Struct. Bonding*, 1987, **68**, 29-87.
4. D. M. P. Mingos, Z. Lin and T. Sree, *Chem. Phys.*, 1990, **142**, 321-334.
5. D. M. P. Mingos, *The Chemical Bond I*, Springer, 2017.
6. D. J. Wales and D. M. P. Mingos, *Inorg. Chem.*, 1989, **28**, 2748-2754.
7. W. D. Knight, K. Clemenger, W. A. de Heer, W. A. Saunders, M. Y. Chou and M. L. Cohen, *Phys. Rev. Lett.*, 1984, **52**, 2141-2143.
8. S. N. Khanna and P. Jena, *Phys. Rev. Lett.*, 1992, **69**, 1664-1667.
9. S. N. Khanna and P. Jena, *Phys. Rev. B*, 1995, **51**, 13705-13716.
10. M. Walter, J. Akola, O. Lopez-Acevedo, P. D. Jazdzinsky, G. Calero, C. J. Ackerson, R. L. Whetten, H. Gronbeck and H. Häkkinen, *Proc. Natl. Acad. Sci. USA*, 2008, **105**, 9157-9162.
11. H. Häkkinen, *Chem. Soc., Rev.*, 2008, **37**, 1847-1859.
12. S. Jin, S. Wang and M. Zhu, *Chem.-Asian J.*, 2019, **14**, 3222-3231.
13. M. W. Heaven, A. Dass, P. S. White, K. M. Holt and R. W. Murray, *J. Am. Chem. Soc.*, 2008, **130**, 3754-3755.
14. X. Kang, H. Chong and M. Zhu, *Nanoscale*, 2018, **10**, 10758-10834.
15. R. S. Dhayal, J.-H. Liao, Y.-C. Liu, M.-H. Chiang, S. Kahlal, J.-Y. Saillard and C. W. Liu, *Angew. Chem. Int. Ed.*, 2015, **54**, 3702-3706.
16. R. S. Dhayal, Y.-R. Lin, J.-H. Liao, Y.-J. Chen, Y.-C. Liu, M.-H. Chiang, S. Kahlal, J.-Y. Saillard and C. W. Liu, *Chem. Eur. J.*, 2016, **22**, 9943-9947.
17. H. Yang, Y. Wang, J. Lei, L. Shi, X. Wu, V. Mäkinen, S. Lin, Z. Tang, J. He, H. Häkkinen, L. Zheng and N. Zheng, *J. Am. Chem. Soc.*, 2013, **135**, 9568-9571.
18. M. Zhu, C. M. Aikens, F. J. Hollander, G. C. Schatz and R. Jin, *J. Am. Chem. Soc.*, 2008, **130**, 5883-5885.

19. J. Akola, M. Walter, R. L. Whetten, H. Häkkinen and H. Gronbeck, *J. Am. Chem. Soc.*, 2008, **130**, 3756-3757.
20. B. K. Teo, H. Zhang and X. Shi, *J. Am. Chem. Soc.*, 1990, **112**, 8552-8562.
21. B. K. Teo, X. Shi and H. Zhang, *J. Am. Chem. Soc.*, 1991, **113**, 4329-4331.
22. R. Hoffmann, *Angew. Chem. Int. Ed. Engl.*, 1982, **21**, 711-724.
23. S. Saito and S. Ohnishi, *Phys. Rev. Lett.*, 1987, **59**, 190-193.
24. L. Cheng and J. Yang, *J. Chem. Phys.*, 2013, **138**, 141101-141104.
25. J. M. Goicoechea and S. C. Sevov, *J. Am. Chem. Soc.*, 2005, **127**, 7676-7677.
26. Z.-M. Sun, H. Xiao, J. Li and L.-S. Wang, *J. Am. Chem. Soc.*, 2007, **129**, 9560-9561.
27. I. Chakraborty and T. Pradeep, *Chem. Rev.*, 2017, **117**, 8208-8271.
28. X. Kang, J. Xiang, Y. Lv, W. Du, H. Yu, S. Wang and M. Zhu, *Chem. Mater.*, 2017, **29**, 6856-6862.
29. B. K. Teo, X. Shi and H. Zhang, *Inorg. Chem.*, 1993, **32**, 3987-3988.
30. P. Jena and Q. Sun, *Chem. Rev.*, 2018, **118**, 5755-5870.
31. A. Muñoz-Castro, *Chem. Commun.*, 2019, **55**, 7307-7310.
32. A. Muñoz-Castro, *Phys. Chem. Chem. Phys.*, 2020, **22**, 1422-1426.
33. B. K. Teo and K. Keating, *J. Am. Chem. Soc.*, 1984, **106**, 2224-2226.
34. Q. Liu, C. Xu, Xia Wu and L. Cheng, *Nanoscale*, 2019, **11**, 13227-13232.
35. D. M. P. Mingos, *Dalton Trans.*, 2015, **44**, 6680-6695.
36. L. Cheng, C. Ren, X. Zhang and J. Yang, *Nanoscale*, 2013, **5**, 1475-1478.
37. L. Liu, P. Li, L.-F. Yuan, L. Cheng and J. Yang, *Nanoscale*, 2016, **8**, 12787-12792.
38. T.-H. Chiu, J.-H. Liao, F. Gam, I. Chantrenne, S. Kahlal, J.-Y. Saillard and C. W. Liu, *J. Am. Chem. Soc.*, 2019, **141**, 12957-12961.
39. F. K. Sheong, J.-X. Zhang and Z. Lin, *Inorg. Chem.*, **55**, 2016, 11348-11353.
40. K. Nunokawa, M. Ito, T. Sunahara, S. Onaka, T. Ozeki, H. Chiba, Y. Funahashi, H. Masuda, T. Yonezawa, H. Nishihara, M. Nakamoto and M. Yamamoto, *J. Chem. Soc., Dalton Trans.*, 2005, 2726-2730.
41. H. Qian, W. T. Eckenhoff, Y. Zhu, T. Pintauer and R. Jin, *J. Am. Chem. Soc.*, 2010, **132**, 8280-8281.
42. E. J. Baerends, T. Ziegler, A. J. Atkins, J. Autschbach, O. Baseggio, D. Bashford, A. Bérces, F. M. Bickelhaupt, C. Bo, P. M. Boerrigter, L. Cavallo, C. Daul, D. P. Chong, D. V. Chulhai, L. Deng, R. M. Dickson, J. M. Dieterich, D. E. Ellis, M. van Faassen, L. Fan, T. H. Fischer, C. Fonseca Guerra, M. Franchini, A. Ghysels, A. Giammona, S. J. A. van Gisbergen, A. Goez, A. W. Götz, J. A. Groeneveld, O. V. Gritsenko, M. Grüning, S. Gusarov, F. E. Harris, P. van den Hoek, Z. Hu, C. R. Jacob, H. Jacobsen, L. Jensen, L. Joubert, J. W. Kaminski, G. van Kessel, C. König, F. Kootstra, A. Kovalenko, M. V. Krykunov, E. van Lenthe, D. A. McCormack, A. Michalak, M. Mitoraj, S. M. Morton, J. Neugebauer, V. P. Nicu, L. Noodleman, V. P. Osinga, S. Patchkovskii, M. Pavanello, C. A. Peebles, P. H. T. Philipsen, D. Post, C. C. Pye, H. Ramanantoanina, P. Ramos, W. Ravenek, J. I. Rodríguez, P. Ros, R. Rüger, P.R.T. Schipper, D. Schlüns, H. van Schoot, G. Schreckenbach, J. S. Seldenthuis,

- M. Seth, J. G. Snijders, M. Solà, M. Stener, M. Swart, D. Swerhone, V. Tognetti, G. te Velde, P. Vernooijs, L. Versluis, L. Visscher, O. Visser, F. Wang, T. A. Wesolowski, E. M. van Wezenbeek, G. Wiesenekker, S. K. Wolff, T. K. Woo and A. L. Yakovlev, ADF2018, SCM, Theoretical Chemistry, Vrije Universiteit, Amsterdam, The Netherlands, 2018.
43. A. D. Becke, *Phys. Rev. A*, 1988, **38**, 3098-3100.
44. J. P. Perdew, *Phys. Rev. B*, 1986, **33**, 8822-8824.
45. E. van Lenthe, E.-J. J. Baerends and J. G. Snijders, *J. Chem. Phys.*, 1994, **101**, 9783-9792.
46. A. Klamt and G. Schüürmann, *J. Chem. Soc., Perkin Trans.*, 2 1993, **105**, 799-805.
47. C. C. Pye and T. Ziegler, *Theor. Chem. Acc.*, 1999, **101**, 396-408.
48. F. Gam, D. Pérez-Hernandez, R. Arratia-Pérez, C. W. Liu, S. Kahlal, J.-Y. Saillard and A. Muñoz-Castro, *Chem. Eur. J*, 2017, **23**, 11330–11337.
49. K. Nobusada, *J. Phys. Chem. C*, 2007, **111**, 14279-14282.
50. R. Jin, C. Liu, S. Zhao, A. Das, H. Xing, C. Gayathri, Y. Xing, N. L. Rosi, R. R. Gil and R. Jin, *Nano*, 2015, **9**, 8530-8536.
51. S. Yang, J. Chai, Y. Lv, T. Chen, S. Wang, H. Yu and M. Zhu, *Chem. Commun.*, 2018, **54**, 12077-12080.
52. S. Yang, J. Chai, T. Chen, B. Rao, Y. Pan, H. Yu and M. Zhu, *Inorg. Chem.*, 2017, **56**, 1771-1774.
53. J. S. Wright, *Can. J. Chem.*, 1973, **51**, 139-146.
54. P. G. Burton and M. D. Harvey, *Nature*, 1977, **266**, 826-827.
55. L. B. Harding and A. W. Goddard III, *J. Chem. Phys.*, 1977, **67**, 2377-2379.
56. B. Flemmig, P. T. Wolczanski and R. Hoffmann, *J. Am. Chem. Soc.*, 2005, **127**, 1278-1285.
57. D. S. Sabirov and I. S. Shepelevich, *Comput Theor. Chem.*, 2015, **1073**, 61–66.
58. E. G. Mednikov and L. F. Dahl, *J. Am. Chem. Soc.*, 2008, **130**, 14813-14821.
59. P. H. Svensson and L. Kloos, *Chem. Rev.*, 2003, **103**, 1649-1684.
60. P. Pyykkö and N. Runeberg *J. Mol. Struct. THEOCHEM*, 1991, **234**, 269-277.
61. Y. Song, F. Fu, J. Zhang, J. Chai, X. Kang, P. Li, S. Li, H. Zhou and M. Zhu, *Angew. Chem. Int. Ed.*, 2015, **54**, 8430-8434.
62. S. Jin, M. Zhou, X. Kang, X. Li, W. Du, X. Wei, S. Chen, S. Wang and M. Zhu, *Angew. Chem. Int. Ed.*, 2020, **132**, 3919–3923.
63. H. Häkkinen, *Chem. Soc. Rev.*, 2008, **37**, 1847-1859.
64. H.-J. Zhai, B. Kiran, J. Li, and L.-S. Wang, *Nature*, 2004, **2**, 827-833.
65. H.-J. Zhai, A. N. Alexandrova, K. A. Birch, A. Boldyrev and L.-S. Wang, *Angew. Chem. Int. Ed.*, 2003, **132**, 6004–6008.